Seismic channel waves in the accretionary prism of the Middle America Trench

N. M. Shapiro[1] and M. Campillo

Laboratoire de Géophysique Interne et Tectonophysique, UA CNRS 733, Université Joseph Fourier, Grenoble, France

S. K. Singh and J. Pacheco

Instituto de Geofísica, Universidad National Autónoma de México, México D.F.

Abstract. A visual examination of seismograms of earthquakes located near the Middle America Trench and recorded on VBB seismographs along the Pacific coast of Mexico, when bandpass filtered between 6 and 30 s, shows the presence of two types of waves. The first is a short pulse and the second is a dispersed wavetrain. The first type of wave is quickly attenuated, while the second type propagates without significant attenuation. We applied a frequency-time analysis to identify the nature of these waves. A comparison of period-group velocity diagrams for signals recorded on different stations shows that the first arrival is a Rayleigh wave propagating in the continental plate, while the second one propagates along the trench in the thickened sediment wedge of the accretionary prism. We have also measured group velocities of Rayleigh wave propagating in the Cocos plate far from the coast. At periods between 15 and 20 s, the group velocities of the wave propagating along the trench are lower than the velocity of Rayleigh waves propagating in adjacent continental and oceanic plates. We conclude that the dispersed wavetrain observed near the coast is a wave trapped in a channel formed by low-velocity sediments of the accretionary prism.

Introduction

Low-velocity zones in the Earth give rise to trapped seismic waves. The waves trapped in low-velocity sedimentary basins provide one example. These basin waves are responsible for amplification of ground motion and damage during earthquakes. For this reason, the computation of response of sedimentary basins excited by earthquakes is a very active field of research (e.g. Bard and Bouchon, 1980; Sánchez-Sesma et al., 1988; Vidale and Helmberger, 1988; Kawase and Aki, 1989). Trapped waves have also been reported in the low-velocity zone formed by subducted oceanic crust (

Fukao et al., 1983) and in the interplate fault zones of California (e.g. Li et al., 1990; Hough et al., 1994; Li et al., 1997).

Basins, generally, have very irregular 3D structure. For this reason, the characteristics of the surface waves propagating in basins change rapidly from one point to next (Frankel, 1994). In the case of a fault zone, the low-velocity wave guide has roughly a 2D structure. Consequently, the signals have some regular characteristics. This permits development of analytical solutions (Ben-Zion and Aki, 1990) and simple numerical algorithms for modeling of these waves (e.g., Cormier and Spudich, 1984; Hori et al., 1985; Li and Leary, 1990; Huang et al., 1995; Li and Vidale, 1996; Igel et al., 1997). Comparison of the results of forward modeling with the observations can be used to infer the fault-zone structure. Ben-Zion (1997) has studied this subject in detail.

Basin waves are excited by the interaction of an incident seismic wave field with a sedimentary basin. The source may be near or, as in the case of the Valley of Mexico, several hundred km away from the basin. So far, the fault-zone trapped waves have been observed only when the source is located in or near the zone. Recent theoretical investigations of Ben-Zion (1997), however, show that these waves can be excited by sources located far from the fault zone.

In this paper we report on surface waves trapped in the accretionary prism of the Middle America Trench (MAT). These waves bear resemblance to both the basin waves and the fault-zone trapped waves. Like the basin waves, these are waves trapped in the superficial low-velocity sediments. However, unlike the case of a typical basin, the accretionary prism has a 2D structure which forms a low-velocity channel. Therefore, surface waves can propagate in this channel for long distances without significant change in their dispersion characteristics. In this sense, these waves are similar to the fault-zone trapped waves.

Data

In recent years, a network of very broadband seismographs has become operational in Mexico. A brief description of this network, which is operated by Insti-
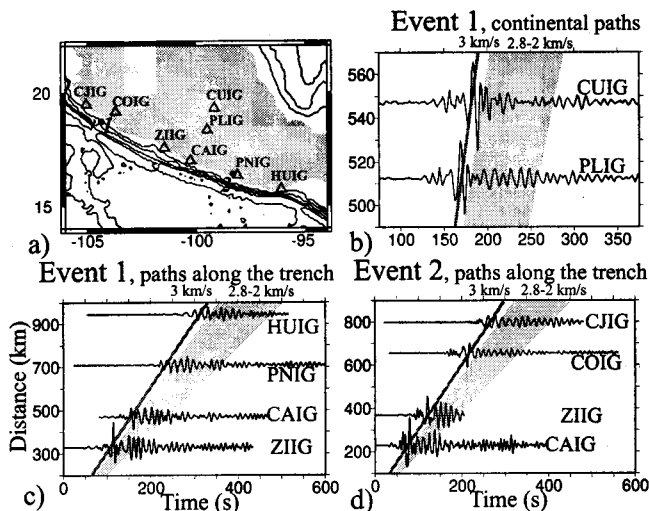
Figure 1. (a) Map of studied region with locations of stations (triangles) and events 1 and 2 (dots). (b)-(d) Z-component seismograms recorded during events 1 and 2 and plotted at the same amplitude scale. Gray lines and shaded areas indicate times corresponding to velocities of continental and trapped Rayleigh waves.

tuto de Geofísica, UNAM, is given in Singh et al. (1997). Six stations of this network are located along the Pacific coast of Mexico (Fig. 1a), covering a distance of about 1000 km. For this study, we selected 11 earthquakes (Table 1). Seven of these are located along the subduction zone, three occurred along the diffuse transform fault boundary between the Rivera and Cocos plates (but close to the trench), and one was located on the east Pacific rise. We use the seismograms of these events at the six coastal stations and two inland stations to study the characteristics of wave propagation along of the Middle America Trench.

Two types of waves near the coast

We begin with a visual inspection of the seismograms recorded during events 1 and 2 (Fig. 1a, Table 1). In Figs. 1b to 1d, we present vertical (Z) component seismograms that have been bandpassed between 6 and 30 sec. Particle motion of vertical and radial component indicates that signals are composed of Rayleigh waves. From Fig. 1 we note that the signal is composed of two arrivals. The first is a short pulse and the second is a slow dispersed wavetrain. We also see two differences between signals propagating along the coast (Figs. 1c and 1d) and along the continental path (Fig. 1b). (1) The amplitude of the slow dispersed wave recorded at PLIG is about 3 times less than the amplitude of the first pulse. For the same event, the amplitudes of the first pulse and the slow wave at CAIG are similar. PLIG and CAIG are located at similar distances from the epicenter. Therefore, in the relative sense, the slow wave is stronger along the coast than along the continental path. (2) The slow wave was not recorded at PLIG

during events 6 and 7. Moreover, such a wave was not recorded at CUIG during event 1. On the other hand, the slow wave is present on coastal records of all events with epicenter lying near the coast or offshore. Therefore, the slow wave propagating along the coast is a stable phenomenon. The same is not true for the continental slow wave. We also note that the first pulse is quickly attenuated along the trench and the dispersed wavetrain dominates at far stations.

Frequency-time analysis

In order to identify the nature of the two arrivals seen on the coastal stations we performed a frequency-time analysis, using a logarithmic stacking technique (Campillo et al., 1996; Shapiro et al., 1997). This method permits selection of arrivals with stable dispersion characteristics. In Fig. 2b we show a stacked period-group velocity, (T-U), diagram of Z component of events 1, 6, and 7 at PLIG. This diagram corresponds to a purely continental path and serves as the reference. The diagram for the same events at the coastal station ZIIG is shown in Fig. 2c. At periods less than 20 s we see two branches at ZIIG. The first one, with a constant velocity of about 3 km/s, is similar to the diagram for the continental path (Fig. 2b), suggesting that it corresponds to a Rayleigh wave propagating in the continental plate. The second branch corresponds to the dispersed wavetrain (Figs 1c and 1d). Similar branch is absent from the diagram at PLIG. This confirms that a slow wave propagating along continental paths is not a stable phenomena.

We considered the events with epicenters close to the trench separately. These events are 4 and 5 recorded at CJIG and events 8, 9, and 10 recorded at CAIG and PNIG (Fig. 2a). On these seismograms the dispersed wavetrain dominates. The characteristics of stacked (T-U) diagram, shown in Fig. 2d, is similar to the second branch in Fig. 2c for periods less than 20s. Finally, we estimated the dispersion of Rayleigh wave propagating in the oceanic Cocos plate, far from the coast, through the stacking of (T-U) diagrams of vertical and radial component of event 11 (out of range of Fig. 2a) at

Table 1. Events used in this study. (∗) The horizontal and vertical errors in the location may be more than 10km.

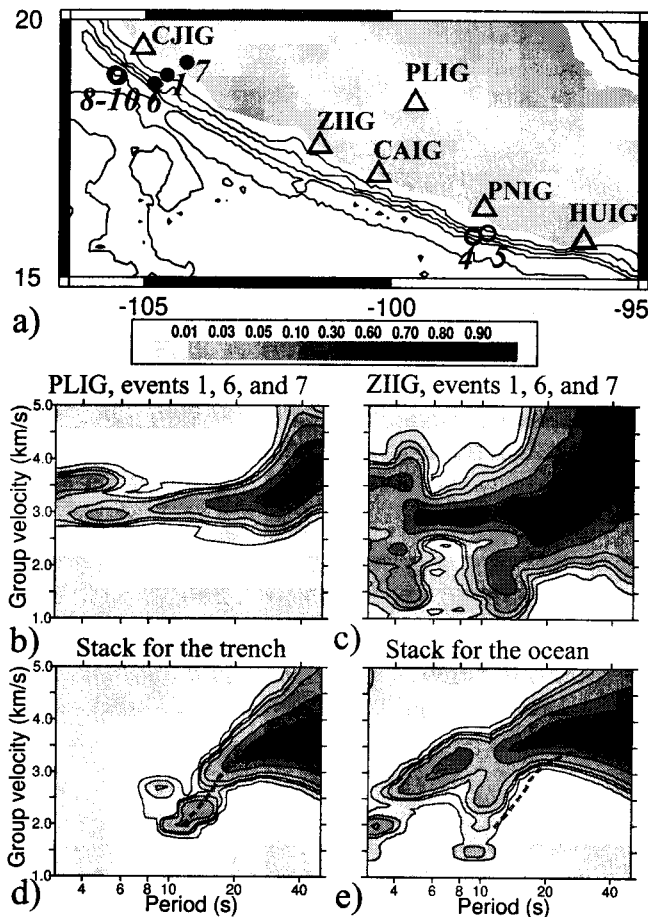| N	Date	Time	Lat*	Long*	H*	M
1	95.10.06	05:13:28	18.77	-104.51	10	5.8
2	97.01.21	21:58:58	16.43	-98.22	5	5.4
3	96.03.27	12:34:48	16.37	-98.30	17	5.4
4	96.02.25	03:08:09	15.63	-98.26	18	7.1
5	96.02.26	01:37:27	15.69	-98.20	19	5.0
6	95.10.10	00:06:16	18.58	-104.60	34	4.9
7	95.10.12	16:52:52	18.71	-104.19	20	5.9
8	95.12.11	14:09:21	18.74	-105.48	9	6.3
9	95.12.11	19:11:41	18.77	-105.53	33	5.4
10	95.12.11	19:44:09	18.74	-105.51	33	6.0
11	95.05.29	09:06:19	10.12	-103.96	10	5.1

Figure 2. Results of frequency-time analysis. (a) Map with locations of stations (triangles) and events used in computing the period-group velocity (T-U) diagrams. (b) and (c) Stacked (T-U) diagrams of Z-component of events 1, 6, and 7 at PLIG and ZIIG. (d) Stacked (T-U) diagram of Z-component of events 4 and 5 at CJIG, and events 8, 9, and 10 at CAIG and PNIG. Dashed line indicates the dispersion curve. (e) Stacked (T-U) diagram of Z- and horizontal components of event 11 (located outside the map in Fig. 2a) at PNIG and HUIG. For comparison, dashed line, from Fig. 2d and corresponding to dispersion curve of the trapped wave in the trench, is also shown.

1961) report 3 km of sediments with a mean P-wave velocity of 3.5 km/s in the MAT near Guatemala. The comparison shows that the inversions of the group velocity curve of the dispersed wavetrain gives reasonable values for the accretionary prism of MAT. Therefore, this wavetrain can be interpreted as a trapped wave in the channel formed by the low-velocity sediments of the accretionary prism of the MAT.

Discussion and Conclusions

We have observed a surface wave propagating along the MAT in the low-velocity accretionary prism. A visual analysis of seismograms shows that the attenuation of this wave is lower than the attenuation of the Rayleigh wave propagating along the coast in the continental plate. This weak attenuation can be explained by the geometry of the accretionary prism which forms a low-velocity channel. The dispersed wavetrain is a wave trapped in this channel. This observation is in agreement with Huang et al. (1995) who simulated wave propagation in a 2D low-velocity channel and found a lower attenuation for waves trapped inside the channel.

The observed surface waves trapped in a low-velocity accretionary prism are similar to the basin waves in as much as the seismic energy is trapped in a superficial low-velocity material in both cases. On the other hand, this wave, which propagates in a 2D low-velocity channel, can be compared with the fault-zone trapped waves. Similar to observations of the fault-zone trapped waves, the waves trapped in the accretionary prism are excited efficiently by sources acting close to the low-velocity zone. In Fig. 3, we present Z-component seismograms of four subduction events recorded at ZIIG and bandpassed between .03 and .15 Hz. We note that the offshore events 4 and 5 give rise to more efficient excitation of trapped waves than the coastal events 2 and 3.

The waves trapped in the accretionary prism can be used to infer the structure of the low-velocity channel. A 1D inversion of the dispersion curve gives reasonable
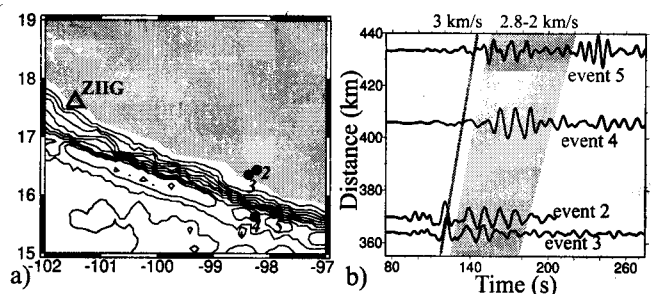
PNIG and HUIG (Fig. 2e). Diagrams in Figs. 2d and 2e have similar features. They have very low velocities at small periods. This leads us to conclude that the dispersed waves observed in the coastal seismograms from coastal and offshore events correspond to propagation along an oceanic path. However, a careful examination shows that at periods around 15 s this wave has a lower velocity (shown by dashed line in Figs. 2d and 2e) as compared to the wave propagating in the ocean far from the coast. A 1D Monte-Carlo inversion of this measured dispersion curve (Shapiro et al., 1997) gives a superficial 2.5 km thick layer with a S-wave velocity of 1.7 km/s.   Kostoglodov et al. (1996) obtained a 3km thick accretionory prism from the modelling of the gravity data in Guerrero, Mexico.   Shor et al. (

Figure 3. (a) Map with bathymetry and location of station ZIIG and , events 2, 3, 4, and 5. (b) Z-component seismograms recorded at ZIIG during events 2, 3, 4, and 5. Gray line and shaded area show times corresponding to velocities of continental and trapped Rayleigh waves.

average values for the sediment thickness and S-wave velocity. However, such 1D model is only a very rough approximation. The channel waves reported here, probably, cannot be explained by simple 1D models used in the studies of the fault-zone trapped waves. The results of 3D modelling could be useful in interpreting the observations in terms of an average 2D trench structure. In any case, the identification of the dispersed wave-train as channel wave along the accretionary prism is important when using coastal seismograms to contruct dispersion curves and in attempts to model the observed waveforms. An immediate application of our observation may be the use of the trapped waves for a rough discrimination between off shore and on shore thrust events. In many cases this improves significantly the earthquake location.

References

Bard, P.-Y., and Bouchon, M., The seismic response of sediment-filled valleys, part I, the case of incident SH-waves, *Bull. Seism. Soc. Am.*, 70, 1263–1286, 1980.

Ben-Zion, Y., and Aki, K., Seismic radiation from an SH line source in a laterally heterogeneous planar fault zone, *Bull. Seism. Soc. Am.*, 80, 971–994, 1990.

Ben-Zion, Y., Properties of seismic fault zone waves and their utility for imaging low velocity structures, *J. Geophys. Res.*, submitted, 1997.

Campillo, M., Singh, S. K., Shapiro, N., Pacheco, J., and Herrmann, R. B., Crustal structure south of the Mexican volcanic belt, based on group velocity dispersion, *Geofis. Intern.*, 35, 361–370, 1996.

Cormier, V., and Spudich, P., Amplification of ground motion and waveform complexity in fault zones: examples from the San Andreas and Calaveras faults, *Geophys. J. R. astr. Soc.*, 79, 135–152, 1984.

Frankel, A., Dense array recording in the San Bernardino valley of Landers-Big Bear aftershocks: basin surface waves, Moho reflections, and three-dimensionnal simulations, *Bull. Seism. Soc. Am.*, 84, 613–624, 1994.

Fukao, Y., Hori, S., and Ukawa, M., A seismological constraint on the depth of basalt-eclogite transition in a subducting oceanic crust, *Nature*, 303, 413–415, 1983.

Hori, S., Inoue, H., Fukao, Y., and Ukawa, M., Seismic detection of the untransformed 'basaltic' oceanic crust subducting into the mantle, *Geophys. J. R. astr. Soc.*, 83, 169–197, 1985.

Hough, S. E., Ben-Zion, Y., and Leary, P. C., Fault-zone waves observed at the southern Joshua Tree earthquake rupture zone, *Bull. Seism. Soc. Am.*, 84, 761–767, 1994.

Huang, B.-S., Teng, T.-L., and Yeh, Y. T., Numerical modeling of fault-zone trapped waves: acoustic case, *Bull. Seism. Soc. Am.*, 85, 1711–1717, 1995.

Igel, H., Ben-Zion, Y., and Leary, P. C., Simulation of SH- and P-SV-wave propagation in fault zones, *Geophys. J. Int.*, 128, 533–546, 1997.

Kawase, H., and Aki, K., A study on the response of a soft basin for incident S, P, and Rayleigh waves with special reference to the long duration observed in the Mexico City, *Bull. Seism. Soc. Am.*, 79, 1361–1382, 1989.

Kostoglodov, V., Bandy, W., Dominguez, J., and Mena, M., Gravity and seismicity over the Guerrero seismic gap, Mexico, *Geophys. Res. Lett.*, 23, 3385–3388, 1996.

Li, Y.-G., and Leary, P. C., Fault zone trapped seismic waves, *Bull. Seism. Soc. Am.*, 80, 1245–1271, 1990.

Li, Y.-G., and Vidale, J. E., Low-velocity fault-zone guided waves: numerical investigation of trapping efficiency, *Bull. Seism. Soc. Am.*, 86, 371–378, 1996.

Li, Y.-G., Leary, P. C., Aki, K., and E.Malin, P., Seismic trapped modes in the Oroville and San Andreas fault zones, *Science*, 249, 763–766, 1990.

Li, Y.-G., Ellsworth, W. L., Thurber, C. H., Malin, P. E., and Aki, K., Fault-zone guided waves from explosions in the San Andreas Fault at Parkfield and Cienega Valley, California, *Bull. Seism. Soc. Am.*, 87, 210–221, 1997.

Sánchez-Sesma, F. J., Cháves-García, F. J., and Bravo, M. A., Seismic response of a class of alluvial valleys for incident SH waves, *Bull. Seism. Soc. Am.*, 78, 83–95, 1988.

Shapiro, N. M., Campillo, M., Paul, A., Singh, S. K., Jongmans, D., and Sánchez-Sesma, F. J., Surface-wave propagation across the Mexican Volcanic Belt and the origin of the long-period seismic-wave amplification in the Valley of Mexico, *Geophys. J. Int.*, 128, 151–166, 1997.

Shor, G. G., Robert, J. R., and Fisher, L., Middle America Trench: seismic refraction studies, *Geol. Soc. America Bull.*, 72, 721–730, 1961.

Singh, S. K., Pacheco, J., Courboulex, F., and Novelo, D. A., Source parameters of the Pinotepa Nacional, Mexico, earthquake of 27 March,1996 (Mw = 5.4) estimated from near-field recordings of a single station, *J. Seismology*, 1, 39–45, 1997.

Vidale, J. E., and Helmberger, D. V., Elastic finite-difference modelling of the 1971 San Fernando, California earthquakes, *Bull. Seism. Soc. Am.*, 78, 122–141, 1988.

N. M. Shapiro, S. K. Singh and J. Pacheco, Departamento de Sismología y Volcanología, Instituto de Geofísica, UNAM, C.P. 04510, México, D.F., México. (e-mail: shapiro@ollin.igeofcu.unam.mx)

M. Campillo, LGIT, IRGIM, BP 53X, F38041, Grenoble CEDEX, France. (e-mail: Michel.Campillo@obs.ujf-grenoble.fr)